FULL PAPER

Dalton
www.rsc.org/dalton

Complexes of a novel multinucleating poly-β-diketonate ligand†

Guillem Aromí,*[a] Christophe Boldron,[b] Patrick Gamez,*[b] Olivier Roubeau,[c] Huub Kooijman,[d] Anthony L. Spek,[d] Helen Stoeckli-Evans,[e] Joan Ribas[a] and Jan Reedijk[b]

[a] *Departament de Química Inorgànica, Universitat de Barcelona, Diagonal 647, 08028 Barcelona, Spain. E-mail: guillem.aromi@qi.ub.es; Fax: +34 93490 7725; Tel: +34 93 402 1264*

[b] *Leiden Institute of Chemistry, Gorlaeus Laboratories, Leiden University, PO Box 9502, 2300 RA Leiden, The Netherlands. E-mail: p.gamez@chem.leidenuniv.nl; Fax: +31 71527 4464; Tel: +31 71527 4671*

[c] *Centre de Recherche Paul Pascal-CNRS UPR8641, 115 avenue du Dr Schweitzer, 33600 Pessac, France*

[d] *Bijvoet Center for Biomolecular Research, Utrecht University, Padualaan 8, 3584 CH Utrecht, The Netherlands*

[e] *Institut de Chimie, Université de Neuchâtel, Avenue de Bellevaux 51, CH-2007 Neuchâtel, Switzerland*

Received 9th July 2004, Accepted 15th September 2004
First published as an Advance Article on the web 29th September 2004

The synthesis of the new polynucleating ligand 1,3-bis-(3-oxo-3-(2-hydroxyphenyl)-propionyl)-benzene (**H_4L**) is reported along with the preparation, structure and properties of its dinuclear complexes $[Cu_2(H_2L)_2(py)_2]$ (**1**), $[Ni_2(H_2L)_2(py)_4]$ (**2**), $[Mn_2(H_2L)_2(dmf)_4]$ (**3**), $[Co_2(H_2L)_2(dmf)_4]$ (**4**) and $[Co_2(H_2L)_2(MeOH)_4]$ (**5**), respectively. In complexes **1** to **5**, the polydentate ligand is in its bis-deprotonated form, chelating the metals through its β-diketonate moieties. Magnetic measurements show that the metals within these molecules are maintained almost mutually independent.

Introduction

The design and synthesis of complicated multidentate ligands with the purpose of creating polynuclear complexes with predetermined functions or structures is increasingly usual in coordination chemistry. This approach has become common practice in such wide contexts as bioinorganic modelling,[1] photochemistry,[2] or that of molecular devices.[3,4] In the area of molecular magnetism, however, this approach has only recently started to take hold.[5] Thus, with a few outstanding exceptions,[6] the majority of systems relevant in the latter context continue to be formed by serendipitous self-assembly,[7] or by rational assembly of building blocks through coordination, using rigid cyanide as bridging ligand.[8] Most of the polydentate ligands designed for the formation of magnetic clusters are based on nitrogen donors. Some structural motifs recreated in this manner are squares,[9] grids[5] or linear chains[10] of closely spaced paramagnetic centers. We have been engaged for some time[11] in the synthesis of new polynucleating ligands possessing oxygen as donating atoms, primarily as poly-β-diketone moieties, aimed at obtaining novel structural motifs in cluster coordination chemistry. A few complexes of poly-β-diketone ligands have been published previously by other groups.[12–14] We recently reported the synthesis of the pentadentate ligand 1,3-bis-(3-oxo-3-phenyl-propionyl)-2-hydroxy-5-methylbenzene (**H_3L′**, see scheme I).[11] The structure of this molecule displays two β-diketone units and one phenol group, disposing five oxygen donor atoms in a linear array, aimed at inducing the aggregation of transition metals in the form of short, molecular chains. The coordination chemistry of this compound has proven very varied, leading to an extensive series of dinuclear,[15] trinuclear,[16,17] octanuclear[18] or one-dimensional infinite species.[19] We describe here the synthesis of a new polynucleating ligand (**H_4L**, see scheme I) based on two β-diketone and two phenol groups. This molecule displays six oxygen donors organized in two arrays of three.

The first complexes of this ligand are a series of dinuclear species with Cu^{II}, Ni^{II}, Mn^{II} and Co^{II}. Their single crystal X-ray structure shows that the ligand is deprotonated preferentially at the diketone units to chelate the metals, the phenol moieties retaining their protons. Therefore, a direct comparison can be established between the series of compounds presented here and the analogous series previously reported with **H_3L′**,[15,17,20] in terms of structure and magnetic properties.

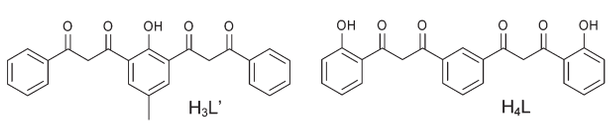

Scheme 1

Experimental

Synthesis

1,3-bis-(3-oxo-3-(2-hydroxyphenyl)–propionyl)–benzene (H_4L). 4 Å molecular sieves (2 g) were activated at 180 °C under vacuum over 2 h in a 500 mL three-necked round-bottom flask. After cooling down to room temperature, a mixture of dimethyl isophthalate (5 g, 25.75 mmol) and 2′-hydroxyacetophenone (6.14 mL, 51.50 mmol) in 290 mL of ethylene glycol dimethyl ether (DME) was added and stirred for 30 min. To this mixture, was carefully added at 4 °C NaH (60% dispersion in mineral oil, 8.24 g, 206 mmol). After completion of the addition, the reaction temperature was gradually raised to that of DME reflux: 15 min at room temperature, 15 min at 50 °C and 30 min at 75 °C. After 20 h refluxing, the reaction mixture was cooled down to room temperature and the precipitate formed was collected by filtration. This solid material was stirred in a mixture of 0.1 M HCl (200 mL) and dichloromethane (DCM; 200 mL). After 1 h of stirring, the organic phase was collected using a separating funnel. The aqueous phase was further extracted twice with DCM (2 × 200 mL). The combined organic layers were dried over Na_2SO_4, filtered and evaporated. The remaining residue was redissolved in refluxing EtOH.

† Electronic supplementary information (ESI) available: Figs. S1 and S2. See http://www.rsc.org/suppdata/dt/b4/b410481a/

DOI: 10.1039/b410481a

Upon cooling, a yellow precipitate (pure $\mathbf{H_4L}$) formed which was filtered and dried under vacuum. The yield was 27%. ESI MS(>0): *m*/*z* 403, $[LH]^+$. ^{1}H NMR ($CDCl_3$, 300 MHz): δ 15.58 (s, 2 H), 12.01 (s, 2 H), 8.48 (s, 1 H), 8.10 (d, 2 H, J = 8 Hz), 7.82 (d, 2 H, J = 8 Hz), 7.63 (t, 1 H, J = 8 Hz), 7.50 (t, 2 H, J = 8 Hz), 7.03 (d, 2 H, J = 8 Hz), 6.96 (t, 2 H, J = 8 Hz), 6.91 (s, 2 H) ppm. Anal. Calcd. (Found) for $\mathbf{H_4L}\cdot 0.5\,H_2O$: C, 70.07 (70.08); H, 4.62 (4.76). ^{13}C NMR ($CDCl_3$, 75 MHz): δ 93.6, 119.7, 120.0, 125.8, 129.4, 130.1, 131.0, 135.2, 137.0, 163.4, 176.7, 196.8 ppm.

$[Cu_2(H_2L)_2(py)_2]$ (1). A mixture of $Cu(OAc)_2\cdot H_2O$ (25 mg, 0.13 mmol) and $\mathbf{H_4L}$ (50 mg, 0.13 mmol) was dissolved in pyridine (10 mL) and stirred for a few minutes. The green solution was layered with toluene and after 10 days, green crystals, suitable for X-ray crystallography, were collected by filtration. The yield was 52%. Anal. Calcd. (Found) for $\mathbf{1}\cdot 3H_2O\cdot 0.5$py: C, 61.60 (61.49); H, 4.31 (3.99); N, 2.97 (3.16).

$[Ni_2(H_2L)_2(py)_4]$ (2). This complex was prepared using the exact same procedure as above using $Ni(OAc)_2\cdot 4H_2O$ (31 mg, 0.13 mmol) as metal salt. The yield was 61%. Anal. Calcd. (Found) for $\mathbf{2}\cdot 0.5H_2O$: C, 65.68 (65.63); H, 4.30 (4.30); N, 4.51 (4.68).

$[Mn_2(H_2L)_2(dmf)_4]$ (3). A mixture of $Mn(OAc)_2\cdot 4H_2O$ (15 mg, 0.06 mmol) and $\mathbf{H_4L}$ (25 mg, 0.06 mmol) was stirred in pyridine (8 mL). Soon after, a yellow precipitate started to form. The mixture was left unperturbed overnight and the solid was then collected by filtration and dissolved in DMF (10 mL). The resulting yellow solution was layered with Et_2O and after 10 days, small crystals of **3**, suitable for X-ray diffraction were collected by filtration. The overall yield was 32%. Anal. Calcd. (Found) for **3**: C, 59.90 (59.62); H, 5.03 (5.28); N, 4.66 (4.59).

$[Co_2(H_2L)_2(dmf)_4]$ (4). This complex was prepared exactly as above, using $Co(OAc)_2\cdot 4H_2O$ (15 mg, 0.06 mmol). The overall yield was 38%. Anal. Calcd. (Found) for $\mathbf{4}\cdot 1.5H_2O$: C, 58.66 (58.45); H, 5.38 (5.16); N, 5.83 (5.80).

$[Co_2(H_2L)_2(MeOH)_4]$ (5). A mixture of $Co(OAc)_2\cdot 4H_2O$ (31 mg, 0.06 mmol) and $\mathbf{H_4L}$ (50 mg, 0.06 mmol) were dissolved in methanol (20 mL) and stirred for 2–3 h. After this, an orange precipitate had formed, which was collected by filtration. The overall yield was 55%. Anal. Calcd. (Found) for **5**: C, 59.66 (60.13); H, 4.62 (4.07).

Physical measurements

Crystals of complexes **1**, **3**, **4** and **5** were placed in the cold nitrogen stream of a Nonius KappaCCD diffractometer on rotating anode. Data for **2** were collected on a Stoe Mark II Image Plate Diffraction System. Details on data collection and structure determination are given in Table 1. Data were collected at 150 K, using Mo Kα radiation (graphite monochromator, λ = 0.71073 Å). No absorption correction was applied. The structures were solved by direct methods (**1**–**4**) or Patterson methods (**5**), using SHELXS86,[21] SHELXS97[22] or DIRDIF.[23] Refinement on F^2 was carried out by full-matrix least-squares techniques using SHELXL97.[24] Hydrogen atom positions were refined (all hydrogens of **2**, hydroxyl hydrogens of **1**, **3** and **5**) or placed at calculated positions, riding on their carrier atoms. All non-hydrogen atoms were refined with anisotropic thermal parameters with the exception of those in the disordered coordinated solvent molecules (**3** and **4**).

CCDC reference numbers: 244348–244352, for **1** to **5**.

See http://www.rsc.org/suppdata/dt/b4/b410481a/ for crystallographic data in CIF or other electronic format.

^{1}H NMR measurements were collected on a 250 MHz Bruker DXR 250 or a 300 MHz Bruker DPX 300 spectrometer in d_6-DMSO and d-$CHCl_3$, respectively. The protio-solvent signals were used as reference and chemical shifts were quoted on the δ scale (down field shifts are positive). Field cooled measurements of the magnetisation of smoothly powdered microcrystalline samples of (**1**, 25.48 mg), (**2**, 17.25 mg), (**3**, 7.10 mg) and (**4**, 8.06 mg) were performed in the range 2–300 K with a Quantum Design MPMS-7XL SQUID magnetometer with an applied field of 1 kG. Corrections for diamagnetic contributions of the sample holder to the measured magnetization and of the sample to the magnetic susceptibility were performed experimentally and by using Pascal's constants, respectively. Elemental analyses were performed in-house on a Perkin Elmer Series II CHNS/O Analyzer 2400, at the Servei de Microanàlisi of CSIC, Barcelona, Spain.

Results and discussion

The synthesis of the new multinucleating ligand $\mathbf{H_4L}$ is an extension of our work aimed at the preparation of magnetic clusters of open-shell metals with structures that would not otherwise be observed. The ligand in scheme I has two well separated groups of oxygen donors, thereby with the potential of gathering independent sets of metals within the same molecule. The presence of four ionizable hydrogen atoms of different acidities (two at the 1,3-diketones and two at the phenol moieties) suggests the possibility of tuning the reactivity of this ligand towards metals by modifying the type and amount of base used in the reaction. The feasibility of this methodology was demonstrated previously with a similar ligand, $\mathbf{H_3L'}$, containing two β-diketone groups as in $\mathbf{H_4L}$, separated by a phenol group. In that case, reactions with the acetate salts of divalent metals (Mn, Co, Ni and Cu) led to the formation of dinuclear complexes where the phenol proton was maintained on the ligand. The increase of the amount and strength of base lead to complete deprotonation of the ligand and formation of complexes with higher nuclearity. The reactivity of $\mathbf{H_4L}$ with $M(OAc)_2$ salts has now been investigated for the divalent metals Cu^{II}, Ni^{II}, Mn^{II} and Co^{II}. In all cases very similar results were obtained, based on the formation of the corresponding dinuclear complexes, where both metals are chelated and bridged by dianionic $\mathbf{H_2L}^{2-}$ through the β-diketone moieties with retention of the phenolic protons. Thus, equimolar amounts of $Cu(OAc)_2$ and $\mathbf{H_4L}$ in pyridine lead to the formation of the complex $[Cu_2(H_2L)_2(py)_2]$ (**1**) according to the reaction in eqn. (1).

$$2Cu(OAc)_2 + 2H_4L + 2py \rightarrow [Cu_2(H_2L)_2(py)_2] + 4AcOH \quad (1)$$

The molecular structure of **1** was determined by single crystal X-ray diffraction (see below), which also provided crystallographic evidence for the identity of $\mathbf{H_4L}$. The analogous reaction with $Ni(OAc)_2$ led to the formation of the related complex $[Ni_2(H_2L)_2(py)_4]$ (**2**), where the preference of Ni^{II} for elongated octahedral geometry is reflected.

When the procedure was repeated with $Mn(OAc)_2$, the formation of a fine yellow precipitate was observed. To crystallize this complex it was redissolved in DMF, from where, crystals of the solvated dimer $[Mn_2(H_2L)_2(dmf)_4]$ (**3**) were obtained, with a geometry very similar to **2**. This complex was of special interest, since among the related dinuclear complexes previously obtained with the ligand $\mathbf{H_3L'}$, the Mn^{II} complex was the only one where $(\mathbf{HL'})^{2-}$ exhibited *syn–anti* conformation of the 1,3-diketonate groups.[15] One possible explanation is that this conformation maximized the energy gained through dipolar contacts within the ligand. This is no longer the case in the absence of the OH from the central phenol group, thus, in complex **3**, the *syn–syn* conformation is restored. This observation supports the initially formulated hypothesis. The exact same procedure with Co^{II} resulted in the formation of the dinuclear complex $[Co_2(H_2L)_2(dmf)_4]$ (**4**). In addition to **4**, the related complex $[Co_2(H_2L)_2(MeOH)_4]$ (**5**) was also synthesized. The preparation of **5** is more convenient than **4** since the former is rather insoluble in MeOH and therefore

Table 1 Crystallographic parameters of complexes **1**, **2**, **3**, **4** and **5**

	1	**2**	**3**	**4**	**5**
Formula	$C_{58}H_{42}Cu_2N_2O_{12}$	$C_{68}H_{50}N_4Ni_2O_{12}\cdot 2(C_5H_5N)$	$C_{60}H_{60}Mn_2N_4O_{16}$	$C_{60}H_{60}Co_2N_4O_{16}$	$C_{52}H_{48}Co_2O_{16}\cdot 2(C_4H_{10}O)\cdot 2(CH_4O)$
FW/g mol^{-1}	1086.04	1390.74	1203.00	1210.98	1259.09
Crystal system	Triclinic	Triclinic	Monoclinic	Monoclinic	Monoclinic
Space group	$P\bar{1}$ (No. 2)	$P\bar{1}$ (No. 2)	$P2_1/c$ (No. 14)	$P2_1/c$ (No. 14)	$P2_1/c$ (No. 14)
a/Å	9.0509(10)	9.0287(7)	33.290(2)	12.0714(16)	8.3075(10)
b/Å	11.566(2)	11.0172(8)	8.8157(10)	8.7556(12)	10.0713(10)
c/Å	11.829(3)	17.3170(12)	50.260(6)	32.284(6)	35.581(5)
α/°	88.556(16)	101.844(6)	—	—	—
β/°	89.026(16)	90.001(6)	131.384(7)	107.321(15)	93.589(12)
γ/°	67.13(2)	105.316(6)	—	—	—
V/Å^3	1140.6(4)	1623.3(2)	11066.9(19)	3257.4(9)	2971.1(6)
$\rho_{calcd.}$/g cm^{-3}	1.581	1.423	1.444	1.235	1.407
Z	1	1	8	2	2
μ(Mo Kα)/mm^{-1}	1.007	0.652	0.532	0.574	0.635
Crystal Color	Green	Pale green	Red–brown	Orange	Orange
Crystal size/mm	0.03 × 0.03 × 0.30	0.10 × 0.27 × 0.36	0.08 × 0.25 × 0.25	0.03 × 0.08 × 0.35	0.1 × 0.3 × 0.3
Total data	29673	23972	135507	37185	33319
Total unique data	5241	8964	20256	5689	5356
R_{int}	0.064	0.036	0.067	0.195	0.076
No. of refined params.	340	563	1502	363	399
*R*1 [a] [$I > 2\sigma(I)$]	0.039	0.035	0.037	0.086	0.046
*wR*2 [b] (all data)	0.092	0.097	0.085	0.229	0.120

[a] $R1 = \Sigma\,||F_o| - |F_c|| / \Sigma\,|F_o|$. [b] $wR2 = (\Sigma w(F_o^2 - F_c^2)^2 / \Sigma w(F_o^2)^2)^{1/2}$.

the synthesis can be carried out in this solvent, from where the product precipitates in high yield. X-ray quality single crystals of **5** had been obtained unexpectedly from a different reaction system before its rational synthesis was laid down.

In light of the complexes obtained from the above reactions, it is important to emphasize the potential of the ligand **H_4L** to coordinate a larger number of metals, *via* the participation of the donor atoms that are still protonated in complexes **1** to **5**. Presumably, this can be achieved during the course of reactions involving larger proportions of metal and in the presence of strong bases. These reactions are currently being explored.

Description of structures

The structures of complexes **1**, **2**, **3** and **5** are represented in Figs. 1 to 5. In Table 1 the crystallographic data for all the complexes are displayed, whereas average selected metric parameters of each complex are in their respective figure legends. The structure details of complex **4** are included as ESI† since its geometry is essentially the same as that of complex **5**.

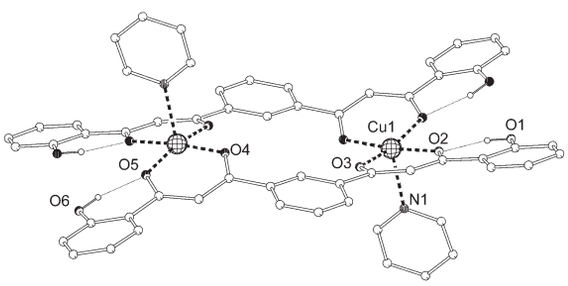

Fig. 1 Molecular drawing of **1**, showing the labelling of unique non-carbon atoms. Only hydrogen atoms bonded to oxygen are shown. Single-lines are hydrogen bonds. Bond and angle ranges (Å and °): Cu–N, 2.317(2); Cu–O, 1.9300(17) to 1.9597(18); N–Cu–O; 91.86(8) to 98.74(7); O–Cu–O(*cis*), 85.40(8) to 92.49(7); O–Cu–O(*trans*), 165.90(7) and 175.65(8); Cu···Cu, 7.539(2).

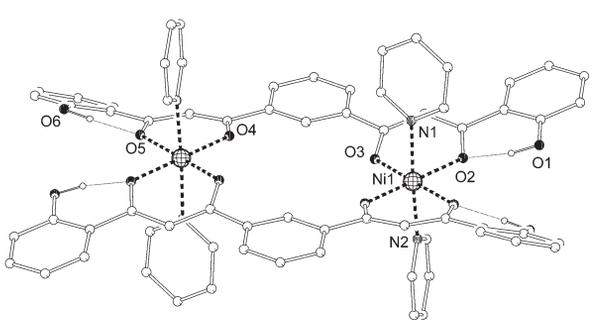

Fig. 2 Molecular drawing of **2**, showing the labelling of unique non-carbon atoms. Only hydrogen atoms bonded to oxygen are shown. Single-lines are hydrogen bonds. Bond and angle (Å and °) ranges: Ni–N, 2.1015(13) and 2.1381(15); Ni–O, 1.9997(14) to 2.0251(10); N–Ni–N, 175.70(5); N–Ni–O, 85.79(5) to 92.17(5); O–Ni–O(*cis*), 88.35(4) to 94.40(4); O–Ni–O(*trans*), 176.24(4) to 176.54(5); Ni···Ni, 7.3226(6).

$[Cu_2(H_2L)_2(py)_2]$ (1). The molecular structure of **1** (Fig. 1) consists of a centrosymmetric dimer containing two Cu^{II} ions bridged and chelated by two H_2L^{2-} ligands through their β-diketonate moieties, which keep the metals 7.539(2) Å apart. The metal ions are thus equatorially coordinated by four O-donors in the form of two opposite six-membered rings. The square pyramidal coordination geometry around copper is completed by axial pyridine ligands pointing to opposite directions from the plane of the molecule. The coplanarity of the coordination pockets within each ligand is gauged by the angle between the corresponding idealized chelate rings, which in **1** measures 23.45(8)°. The structure of **1** reveals the fact that **H_4L** is preferentially deprotonated at the methylene positions between the carbonyl groups of the β-diketone fragments, presumably because the ensuing metal–ligand coordination moiety is very stable, and also because this allows the

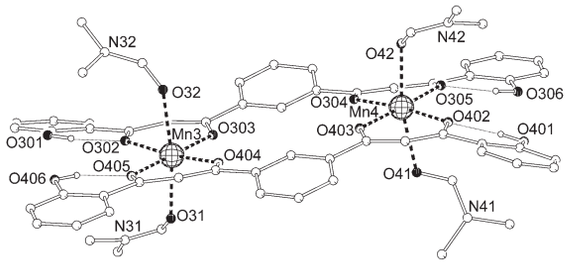

Fig. 3 Molecular drawing of **3**. Only the molecule located at a general position is depicted. Only hydrogen atoms bonded to oxygen are shown. Single-lines are hydrogen bonds. Bond and angle ranges (Å and °, including the three independent molecules in the unit cell, see text): Mn–O(dmf), 2.213(2) to 2.301(3); Mn–O(H_2L), 2.082(2) to 2.151(2); O(dmf)–Mn–O(dmf), 167.65(10) to 170.56(10); O–Mn–O(*trans*), 173.79(8) to 178.73(8); O(dmf)–Mn–O(*cis*), 83.05(9) to 99.69(9); O–Mn–O(*cis*), 84.19(9) to 98.17(9); Mn1···Mn1a, 7.5401(12); Mn2···Mn2a, 7.6433(12); Mn3···Mn4, 7.6092(12).

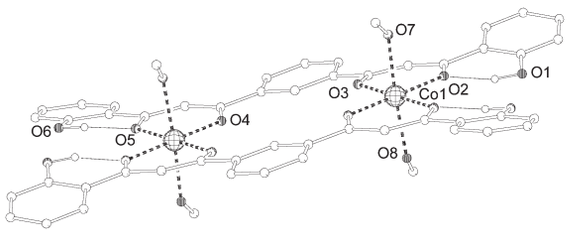

Fig. 4 Molecular drawing of **5**, showing the labelling of unique non-carbon atoms. Only hydrogen atoms bonded to oxygen are shown. Single-lines are hydrogen bonds. Bond and angle (Å and °) ranges: Co–O(MeOH), 2.103(2) and 2.128(2); Co–O(H_2L), 2.0272(19) to 2.0591(19); O(MeOH)–Co–O(MeOH), 176.09(9); O(MeOH)–Co–O, 87.30(8) to 92.57(9); O–Co–O(*cis*), 87.18(8) to 93.57(8); O–Co–O(*trans*), 179.05(8) and 179.16(8); Co···Co, 7.411(1).

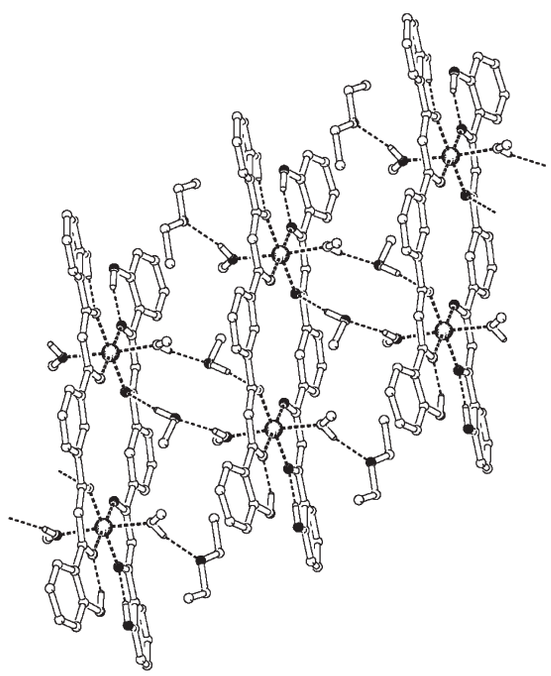

Fig. 5 Representation of complex **5**, emphasizing the hydrogen-bonding network within the crystal lattice, involving MeOH and Et_2O of crystallization. Hydrogen atoms not involved in hydrogen bonding were omitted for clarity.

formation of four hydrogen bonds between the phenol groups and their adjacent oxygen atoms, respectively (Fig. 1). The hydrogen atoms participating in these weak interactions have been found crystallographically, and the corresponding O–H···O distances are 2.590(3) and 2.525(3) Å. The structure of **1** can be directly compared to that of the complex $[Cu_2(HL')_2(dmf)_2]$, reported previously.[20] In the latter, the solvate ligands are dimethylformamide molecules instead of pyridine. The main

difference between both complexes is the distribution of intramolecular hydrogen bonds, as a consequence of the different location and number of phenol groups within the ligand. In the complex with $\mathbf{H_3L'}$, the ligand has only one phenol group separating both diketone units, which participates in one intramolecular hydrogen bond upon formation of the complex. This has a small structural effect, the Cu^{II} ions being only 0.16 Å further apart than in **1**. The packing of the molecules of **1** within the crystal takes place through extensive π-stacking between the phenyl rings from $\mathbf{H_2L}^{2-}$ ligands and chelate rings involving the β-diketonate groups of adjacent molecules. The shortest distances between the centroids of the interacting π systems are 3.50 Å.

$[Ni_2(H_2L)_2(py)_4]$ (2). The molecular structure of **2** (Fig. 2) is similar to that of **1** in that two $\mathbf{H_2L}^{2-}$ ligands bridge two M^{II} ions (here, Ni^{II}) through the chelating diketonate units. The main difference is the fact that solvation of the vacant coordination sites of the metals takes place now at both axial positions, leading to the usual distorted octahedral coordination geometry of Ni^{II}. The separation between Ni^{II} ions is 7.3226(6) Å, whereas the idealized six member chelate rings within a ligand form an angle of 16.73(5)°, considerably smaller than in **1**. The O–H···O distances of the intramolecular hydrogen bonds are 2.5273(16) and 2.5068(16) Å, respectively. Complex **2** is structurally related to the previously reported complex $[Ni_2(HL')_2(py)_4]$.[15] Perhaps the most striking aspect of this comparison is that in the complex with $(\mathbf{HL'})^{2-}$, the metal ions are 0.6 Å further apart than in **2**.

$[Mn_2(H_2L)_2(dmf)_4]$ (3). The structure of **3** (Fig. 3) was quite revealing in that it shows two Mn^{II} ions linked through chelation of both metals by each of two $\mathbf{H_2L}^{2-}$ ligands displaying *cis–cis* conformation. This is the same conformation as in complexes **1** and **2**, but is in contrast with the congener of **3** with $\mathbf{H_3L'}$, $[Mn_2(HL')_2(py)_4]$, where the ligand is found in the *syn–anti* conformation.[15] In both complexes, Mn^{II} is in a distorted octahedral geometry. However, the ligand conformation defines whether the metal configuration is *trans* (complex **3**, with dmf axial ligands) or *cis* ($[Mn_2(HL')_2(py)_4]$). The cause of the conformation in the latter complex is likely to be the stabilization energy provided by the additional hydrogen bonds that are allowed within $(\mathbf{HL'})^{2-}$ in this configuration. Such hydrogen bonds are not possible with $\mathbf{H_4L}$, thus all complexes formed with this ligand exhibit the *cis–cis* form. The determination of the structure of **3** constituted an interesting crystallographic problem, since the crystals were twinned and the structure could only be refined by applying a pseudomerohedral twin operation. The lattice contains three independent molecules of **3**, two located on inversion centers and one on a general position. Therefore, three different Mn···Mn distances are found, 7.5401(12), 7.6433(12) and 7.6092(12) Å. Likewise, four unique values of the angle between chelate rings within the same ligand are found, namely, 8.67(11), 9.90(11), 7.15(11) and 7.99(11). The intramolecular O–H···O distances are all within the range of 2.510 to 2.576 Å. The main differences between the different molecules of **3** in the unit cell are the orientations of the axial dmf molecules. There are no significant packing forces in the crystal structure other than van der Waals' interactions.

$[Co_2(H_2L)_2(MeOH)_4]$ (5). Complex **5** (Fig. 4) is a dinuclear centrosymmetric complex of Co^{II} ions bridged and equatorially coordinated by two $\mathbf{H_2L}^{2-}$ ligands, in the same fashion as in the previous complexes. The solvate axial ligands that complete the elongated octahedral geometry around cobalt are MeOH molecules. The intermetallic distance is 7.4106(12) Å, while the complex shows the smallest angle of the series between both chelate rings within each ligand, which measures 2.54(9)°. While inspection of this pair of parameters for the different compounds studied revealed the absence of any correlation between the two, the angle between chelate rings seems to be related to the nature of the terminal axial ligand (see below). The O–H···O distances of the intramolecular hydrogen bonds are 2.533(3) and 2.519(3) Å. In the solid state, a co-operative hydrogen bond network joins the complex molecules into an infinite, one-dimensional chain, through the intermediacy of solvent molecules of crystallization (Fig. 5). In this network, O4 of the ligand accepts a hydrogen bond from free methanol, while O7 (from coordinated MeOH) acts as a proton donor to the free methanol. Again, complex **5** has its counterpart with the ligand $\mathbf{H_3L'}$, this time in the form of the molecule $[Co_2(HL')_2(py)_4]$.[25]

Comparison of the above structures allows one to observe a possible relation between the angle between the least-squares planes through the chelate rings within one ligand and the identity of the axial ligand, with the following ordering: pyridine (23.45, 16.73) > dmf (8.67, 9.90, 7.15, 7.99, 6.3) > MeOH (2.54). Inspection of these parameters for the corresponding complexes with $(\mathbf{HL'})^{2-}$ reveals that these trends are maintained in this family of compounds. Thus these angles are 29.63 and 30.56 for complexes $[M_2(HL')_2(py)_4]$ (M^{II} = Ni^{II} and Co^{II}),[15] respectively, and 14.59 for $[Cu_2(HL')_2(dmf)_2]$.[20] The reasons for this trend are currently unclear, although they could be of steric nature, given the correlation between the angle and the size of the ligand.

Magnetic properties

Bulk magnetic susceptibility measurements were performed for complexes **1** to **4** in the 2 to 300 K temperature range under a constant magnetic field of 0.1 T. The results are represented together as $\chi_m T$ *vs.* T plots (where χ_m is the molar paramagnetic susceptibility) in Fig. 6, after correction for contributions.

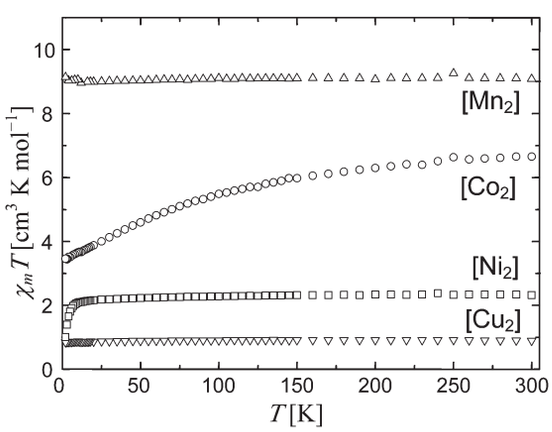

Fig. 6 Plots of $\chi_m T$ *vs.* T per molecule for complexes **1** to **4**.

The value of $\chi_m T$ at 300 K for $[Cu_2(H_2L)_2(py)_2]$ (**1**) is 0.9 cm^3 K mol^{-1}, which corresponds to the value of two independent Cu^{II} ions (S = 1/2) with g = 2.19. The isotropic g value, as extracted from X-band powder EPR at 77 K is 2.17 (Fig. S1, see ESI†). $\chi_m T$ remains constant over the whole temperature range indicating that $\mathbf{H_2L}^{-2}$ does not mediate any detectable magnetic superexchange between the metals of the molecule. This is in contrast to the related complex $[Cu_2(H_2L')_2(dmf)_2]$, where a small interaction between the metals was found of $J = -0.73$ cm^{-1} (with the $\boldsymbol{H} = -2J\boldsymbol{S}_1\boldsymbol{S}_2$ convention for the Heisenberg–Spin Hamiltonian).[19] Presumably, this is allowed by the central phenol group of $(\mathbf{HL'})^{-2}$ (see Scheme I), which forms a hydrogen bond to one oxygen atom bound to Cu^{II} and is absent in $\mathbf{H_2L}^{-2}$. This observation underscores the feasability of modifying the magnetic properties within transition metal assemblies by introducing small modifications on polynucleating ligands.

The complex $[Ni_2(H_2L)_2(py)_4]$ (**2**) exhibits a room temperature value of $\chi_m T$ of 2.32 cm^3 K mol^{-1}, which would be expected for two uncoupled octahedral Ni^{II} centers (S = 1) with g = 2.15. This value stays constant as the temperature is decreased and drops abruptly only at temperatures below 20 K approximately.

In light of the observations from **1**, we exclude antiferromagnetic coupling between Ni^{II} centers as the reason for this drop. Instead, the decrease of $\chi_m T$ is likely to be caused by zero field splitting (ZFS) of the spin ground state of the individual ions. An assessment of the magnitude of the ZFS parameter that would cause the decrease of $\chi_m T$ was made by fitting the data to an equation containing the term D.[26] The best fit (Fig. S2, see ESI†) was found for $D = 6.8\ cm^{-1}$.

Consistent with the above observations, $\chi_m T$ for $[Mn_2(H_2L)_2(dmf)_4]$ (**3**) remains constant at approximately 9.1 $cm^3\ K\ mol^{-1}$ over the whole temperature interval studied. This value is that calculated for two non-interacting high-spin Mn^{II} centers ($S = 5/2$) with $g = 2.04$, which falls within the range commonly observed for this ion. Again, these observations show that **H_4L** is capable of assembling two paramagnetic centers within the same molecule, keeping them magnetically isolated from each other.

The variable temperature magnetic susceptibility of $[Co_2(H_2L)_2(dmf)_4]$ (**4**) is markedly different than that observed for complexes **1** to **3**, as is evident from Fig. 6. The value of $\chi_m T$ at 300 K is 6.65 $cm^3\ K\ mol^{-1}$, which is higher than expected for the presence in one molecule of two isolated spin-only Co^{II} centers with $S = 3/2$. Such a high value is observed because, in fact, the spin angular momentum in this ion is coupled with the orbital angular momentum. The continuous drop of the product $\chi_m T$ taking place with decreasing temperature is the consequence of the depopulation of states of higher magnetic moment within the term $^4T_1$ of Co^{II}. This drop is therefore not ascribed to any antiferromagnetic exchange within the dinuclear complex and leads to a value for $\chi_m T$ of 3.46 $cm^3\ K\ mol^{-1}$ at 2 K.

Paramagnetic ^{1}H NMR

Complexes **1** to **5** were examined by 250 MHz ^{1}H NMR spectroscopy. Of all of them, only the Co^{II} compounds could be prepared in enough concentration or provided suitable spectra. The other complexes were either too insoluble (**1** and **2**) or the resonances where too broad to be detected (**3**). Paramagnetic ^{1}H NMR on synthetic coordination clusters of Co^{II} has been employed occasionally to investigate their properties in solution.[27] Also, this technique has been very useful for obtaining crucial structural information from metalloproteins containing this ion or its analogues.[28]

In Fig. 7 is the spectrum of $[Co_2(H_2L)_2(dmf)_4]$ (**4**) in d_6-DMSO at room temperature, whereas in Table 2 is a list of the chemical shifts observed. The spectrum shows nine paramagnetically shifted and broadened peaks as expected for complex **4** with D_{2h} symmetry in solution. Of these, the two most broadened and shifted (labelled as *c*) are assigned to the protons lying closest to Co^{II}, namely, the phenol and the methine groups of the ligand. The remaining signals were associated to the aromatic protons from $\mathbf{H_2L}^{2-}$, of which the two with apparently half intensity (labelled as *b*) were attributed to the two inequivalent H atoms on the central ring. The other five are labelled as *a*. Of the peaks in the diamagnetic area, the signals from free solvents present in the system (DMSO, H_2O, Et_2O and DMF) were identified by their chemical shifts (see Fig. 7 and Table 2). Two signals in the vicinity of 8 and 4 ppm, respectively where assigned to the two inequivalent 'CH_3' groups from bound dimethylformamide. These two groups are magnetically inequivalent because of the double bond character of the C–N bond in this ligand, which prevents free rotation around this vector. Other examples of this asymmetry, manifested by paramagnetic ^{1}H NMR of complexes containing this solvent-ligand have been observed.[29] This assignment in complex **4** is supported by the fact that the ^{1}H NMR spectrum (not shown) of the related complex **5** (which does not contain dmf) is almost identical to that in Fig. 7, but does not show the peaks attributed to dmf. The aldehyde proton of the ligand dmf is expected to be too broad to be detected. These results suggest that complexes **4** and **5** are maintained in solution with the idealized D_{2h} symmetry observed in the solid state. Such a conclusion fuels the prospect of using these compounds in solution as building blocks for further reactivity. For example, larger composite entities could be grown in this manner by exploiting the potential of the "unused" phenol moieties to bind other substrates, such as other metals or even more complicated building blocks. The study of the reactivity of these complexes with various sources of lanthanide ions is currently in progress.

Table 2 250 MHz ^{1}H NMR data of $[Co_2(H_2L)_2(dmf)_4]$ (**4**) in d_6-DMSO

Resonance	δ/ppm
a (5 resonances)	32.1, 27.9, 19.0, 16.2, 14.6
b (2 resonances)	29.9, 26.7
c (2 resonances)	97, 81
dmf (ligand, 2 resonances)	7.7 or 8.0,[a] 4.3

[a] This resonance comes together with another from free solvent.

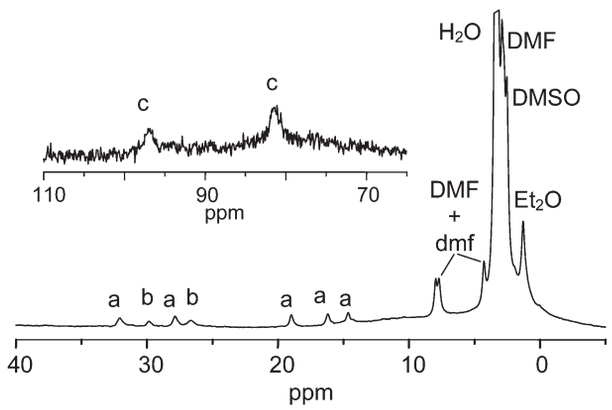

Fig. 7 250 MHz ^{1}H NMR spectrum of $[Co_2(H_2L)_2(dmf)_4]$ (**4**) in d_6-DMSO. The top of the full spectrum has been cropped for clarity. The inset is a magnified (arbitrary intensity units) portion of the region of lowest fields. See text for details about the labels.

Conclusions

The preparation of the first M^{II} complexes of the new polynucleating ligand **H_4L** has revealed that the latter loses preferentially H^+ from its β-diketonate units rather than from the phenol groups. The ensuing dinuclear compounds conserve, unlike previously observed for the related ligand **H_3L′**, the same ligand conformation throughout complexes with Cu^{II}, Ni^{II}, Mn^{II} and Co^{II}, namely, *syn*,*syn* with respect to the β-diketonate groups. In complexes **1** to **4**, both paramagnetic centers are magnetically independent from each other. Work is in progress in order to isolate complexes of **H_4L** with higher metal loading, by using bases capable of ionizing the phenolic 'OH' moieties of this ligand.

Acknowledgements

The authors are thankful to the Spanish Ministerio de Ciencia y Tecnología ("Ramón y Cajal" contract to GA and Grant BQU2003/0539 to JR), to the Dutch WFMO (Werkgroep Fundamenteel-Materialen Onderzoek) (PG, CB and JR) CW (Foundation for the Chemical Sciences) and NWO (Organization for the Scientific Research) (PG, JR, CB and ALS), to the French CNRS (Centre National de la Recherche Scientifique), to the Conseil Général d'Aquitaine, (OR) and to the Swiss National Science Foundation (HS-E) for financial support.

References

1 R. H. Bode, J. E. Bol, W. L. Driessen, F. B. Hulsbergen, J. Reedijk and A. L. Spek, *Inorg. Chem.*, 1999, **38**, 1239.
2 S. Campagna, S. Serroni, F. Puntoriero, F. Loiseau, L. De Cola, C. L. Kleverlaan, J. Becher, A. P. Sorensen, P. Hascoat and N. Thorup, *Chem. Eur. J.*, 2002, **8**, 4461.

3 M. Fujita, K. Umemoto, M. Yoshizawa, N. Fujita, T. Kusukawa and K. Biradha, *Chem. Commun.*, 2001, 509.
4 V. Balzani, A. Credi and M. Venturi, *Chem. Eur. J.*, 2002, **8**, 5524.
5 L. Zhao, Z. Q. Xu, L. K. Thompson and D. O. Miller, *Polyhedron*, 2001, **20**, 1359.
6 E. Breuning, M. Ruben, J. M. Lehn, F. Renz, Y. Garcia, V. Ksenofontov, P. Gütlich, E. Wegelius and K. Rissanen, *Angew. Chem., Int. Ed.*, 2000, **39**, 2504.
7 R. E. P. Winpenny, *J. Chem. Soc., Dalton Trans.*, 2002, 1.
8 V. Marvaud, C. Decroix, A. Scuiller, C. Guyardduhayon, J. Vaissermann, F. Gonnet and M. Verdaguer, *Chem. Eur. J.*, 2003, **9**, 1677.
9 D. S. Cati, J. Ribas, J. Ribas-Arino and H. Stoeckli-Evans, *Inorg. Chem.*, 2004, **43**, 1021.
10 C. J. Matthews, S. T. Onions, G. Morata, L. J. Davis, S. L. Heath and D. J. Price, *Angew. Chem., Int. Ed.*, 2003, **42**, 3166.
11 G. Aromí, P. Gamez, P. Carrero, W. L. Driessen and J. Reedijk, *Synth. Commun.*, 2003, **33**, 11.
12 N. A. Bailey, D. E. Fenton, J. Lay, P. B. Roberts, J.-M. Latour and D. Limosin, *J. Chem. Soc., Dalton Trans.*, 1986, 2681.
13 V. A. Grillo, E. J. Seddon, C. M. Grant, G. Aromí, J. C. Bollinger, K. Folting and G. Christou, *Chem. Commun.*, 1997, 1561.
14 R. W. Saalfrank, N. Low, S. Trummer, G. M. Sheldrick, M. Teichert and D. Stalke, *Eur. J. Inorg. Chem.*, 1998, 559.
15 G. Aromí, P. Gamez, O. Roubeau, P. Carrero, H. Kooijman, A. L. Spek, W. L. Driessen and J. Reedijk, *Eur. J. Inorg. Chem.*, 2002, 1046.
16 G. Aromí, P. Carrero, P. Gamez, O. Roubeau, H. Kooijman, A. L. Spek, W. L. Driessen and J. Reedijk, *Angew. Chem., Int. Ed.*, 2001, **40**, 3444.
17 G. Aromí, P. Gamez, O. Roubeau, P. Carrero, H. Kooijman, A. L. Spek, W. L. Driessen and J. Reedijk, *Inorg. Chem.*, 2002, **41**, 3673.
18 G. Aromí, P. Gamez, O. Roubeau, H. Kooijman, A. L. Spek, W. L. Driessen and J. Reedijk, *Angew. Chem., Int. Ed.*, 2002, **41**, 1168.
19 G. Aromí, J. Ribas, P. Gamez, O. Roubeau, H. Kooijman, A. L. Spek, S. Teat, E. MacLean, H. Stoeckli-Evans and J. Reedijk, *Chem., Eur. J.*, 2004 in press.
20 H. Kooijman, A. L. Spek, G. Aromí, P. Gamez, P. Carrero-Berzal, W. L. Driessen and J. Reedijk, *Acta Crystallogr.*, 2002, **E58**, m223.
21 G. M. Sheldrick, in *SHELXS86 Program for Crystal Structure Determination*, Germany, 1986.
22 G. M. Sheldrick, in *SHELXS97 Program for Crystal Structure Determination*, Germany, 1997.
23 P. T. Beurskens, G. Admiraal, G. Beurskens, W. P. Bosman, S. García-Granda, R. O. Gould, J. M. M. Smits, and C. Smycalla, *The DIRDIF99 program system, Technical Report of the Crystallography Laboratory*, University of Nijmegen, The Netherlands, 1999.
24 G. M. Sheldrick, in *SHELXS86 Program for Crystal Structure Refinement*, Germany, 1997.
25 Unpublished results.
26 O. Kahn, *Molecular Magnetism*, VCH, New York, 1993, p. 17.
27 G. Aromí, A. S. Batsanov, P. Christian, M. Helliwell, O. Roubeau, G. A. Timco and R. E. P. Winpenny, *Dalton Trans.*, 2003, 4466.
28 J. Salgado, A. P. Kalverda, R. E. M. Diederix, G. W. Canters, J. M. Moratal, A. T. Lawler and C. Dennison, *J. Biol. Inorg. Chem.*, 1999, **4**, 457.
29 G. Aromí, PhD Thesis, Indiana University, Bloomington, IN, 1999.